

FOURTEENTH EUROPEAN ROTORCRAFT FORUM

Paper No. 62

AGUSTA METHODOLOGY FOR PITCH LINK LOADS
PREDICTION IN PRELIMINARY DESIGN PHASE

F. NANNONI - A. STABELLINI

COSTRUZIONI AERONAUTICHE G. AGUSTA
CASCINA COSTA, SAMARATE, VARESE, ITALY

20-23 September, 1988
MILANO, ITALY

ASSOCIAZIONE INDUSTRIE AEROSPAZIALI
ASSOCIAZIONE ITALIANA DI AERONAUTICA ED ASTRONAUTICA

AGUSTA METHODOLOGY FOR PITCH LINK LOADS
PREDICTION IN PRELIMINARY DESIGN PHASE

by

Fabio NANNONI , Alessandro STABELLINI
PRELIMINARY DESIGN ENGINEERS
COSTRUZIONI AERONAUTICHE G. AGUSTA
CASCINA COSTA, SAMARATE, VARESE, ITALY

ABSTRACT

The fast increase of static and torsional loads at the root of the blade is, sometimes, the first limit that a helicopter meets in forward flight at high speed.

A good design cannot leave out of account, hence, an analysis of this phenomenon that is very important in rotating controls development and, above all, in performances and handling qualities estimation of the whole aircraft.

In this paper will be presented the AGUSTA methodology for the estimation of these loads in the preliminary design phase.

1. INTRODUCTION

The evaluation of the torsional loads at the root of the blade of an helicopter in forward flight is, surely, a very difficult task.

This problem can be resolved, naturally, using sophisticated and very complex computer codes but, today, AGUSTA has a methodology that can allow a good estimation of these loads in the preliminary phase of the design when the necessity of making parametric studies and the small quantity of data available makes very difficult, or even impossible, the use of particularly complex methods.

For these reasons the AGUSTA's "PRELIMINARY DESIGN DEPARTMENT" has thought and developed an algorithm that, also with all the necessary approximations and reductions of the physical and dynamic problems present in the analysis, was endowed with a good flexibility of use and with all of those characteristics that are considered essential for a good calculation of the torsional loads at the root of the blade (a good inflow model, unsteady aerodynamic).

We have to underline that the program was created paying attention to its cost/effectiveness ratio and it is well applicable to conventional configurations of hubs like full articulated ones or, better, with elastomeric bearings.

LIST OF SYMBOLS

- \vec{V} = speed vector in the used frame
- θ_0 = collective pitch
- θ_{90} = longitudinal cyclic pitch
- θ_{00} = longitudinal cyclic pitch
- a_0 = coning angle
- a_1 = longitudinal flapping angle
- b_1 = lateral flapping angle
- ω = rotor angular speed
- t = time
- ψ = azimuth angle
- β = flapping angle
- ρ = air density
- n_B = number of blades
- ϕ = inflow angle
- α = attack angle
- C_L = lift coefficient
- C_D = drag coefficient
- C_M = moment coefficient
- $c(r)$ = local chord
- c_0 = static lead-lag angle
- c_1 = part in $\cos \psi$ of lead-lag angle
- d_1 = part in $\sin \psi$ of lead-lag angle
- r = local radial station
- R = rotor radius
- v_f = local flapping velocity
- v_i = local induced velocity

$S(r)$ = local twist
 T = thrust
 H = H-force of the rotor
 Y = Y-force of the rotor
 Q = torque
 M_{--} = pitch moment at blade root due to any action
 e = hinges offset (% R)
 x_{CG} = radial position of blade center of gravity (% R)
 J = moment of inertia
 M_{BL} = blade mass
 K = damper characteristic
 R_{DR} = lagging hinge stiffness
 N_A = lagging aerodynamic moment
 η = lead-lag angle
 δ = mass for unity of length of blade
 g = acceleration of gravity
 m = distance between aerodynamic center and pitch axes of the blade element (chordwise)
 n = distance between aerodynamic center and center of gravity of the blade element (chordwise)
 F_D = force due to damper
 b_D = damper arm

SUBSCRIPTS AND OTHER SYMBOLS

NF = NO-FEATHER system

SH = SHAFT system

BL = BLADE system

FL = flapping motion

DR = lagging motion

i = blade element indicator

• = d / dt

•• = d² / dt²

2. SIMPLIFIED MATHEMATICAL MODEL

NFCTLL program, here presented, is a "BLADE ELEMENT CODE"; this kind of algorithm was chosen for its particular flexibility and for its good capability of estimation of aerodynamic and dynamic loads.

The program can evaluate, knowing the control angles at 75% of radius and the components of flight speed with respect to the "SHAFT AXES", the forces, the moments, the flapping and lagging motions of a rotor anyhow placed in the space.

2.1 FRAMES OF REFERENCE SELECTION

The calculation of flapping motion and forces is conducted in iterative way. To make this process more stable and quick, all the evaluations are performed in the "NO-FEATHER" system respect to which the cyclic variations of pitch are zero.

Then we are able to write the transformation matrix that allows to pass from the "SHAFT" system to the "NO-FEATHER" frame.

$$[A] = \left\{ \begin{array}{ccc} C_{90} & 0 & -S_{90} \\ \Delta_{\theta} S_{90} C_{90} S_{00} & \Delta_{\theta} C_{00} & \Delta_{\theta} C_{90}^2 S_{00} \\ \Delta_{\theta} S_{90} C_{00} & -\Delta_{\theta} C_{90} S_{00} & \Delta_{\theta} C_{90} C_{00} \end{array} \right\}$$

Where:

$$\Delta_{\theta} = \sqrt{1 - \sin^2 \theta_{90} * \sin^2 \theta_{00}}$$

θ_{90} = Longitudinal cyclic pitch

θ_{00} = Lateral cyclic pitch

$S_{90} = \sin \theta_{90}$

$C_{90} = \cos \theta_{90}$

$S_{00} = \sin \theta_{00}$

$C_{00} = \cos \theta_{00}$

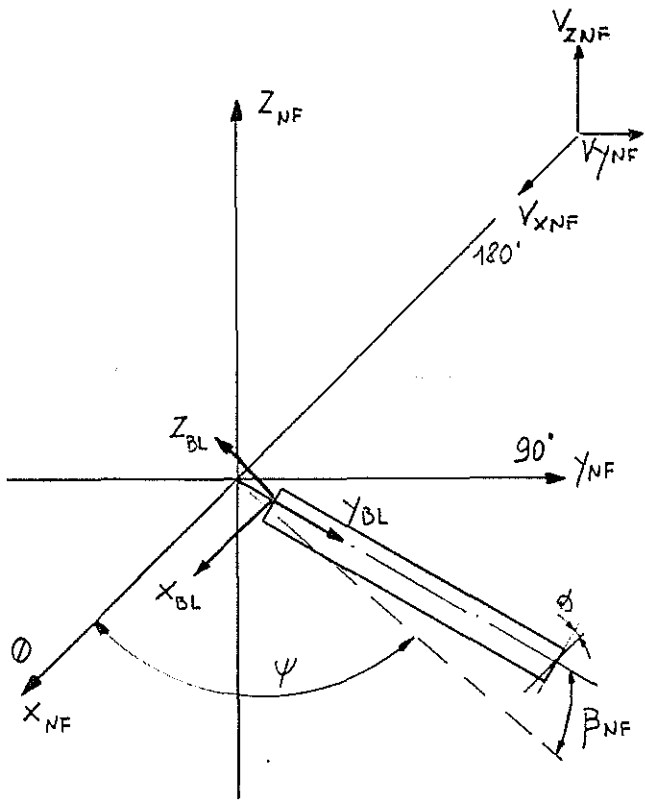


FIG. 1

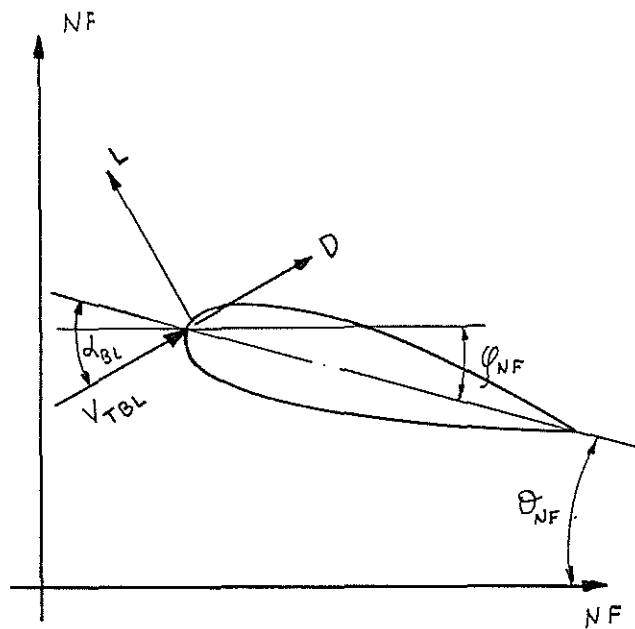


FIG. 2

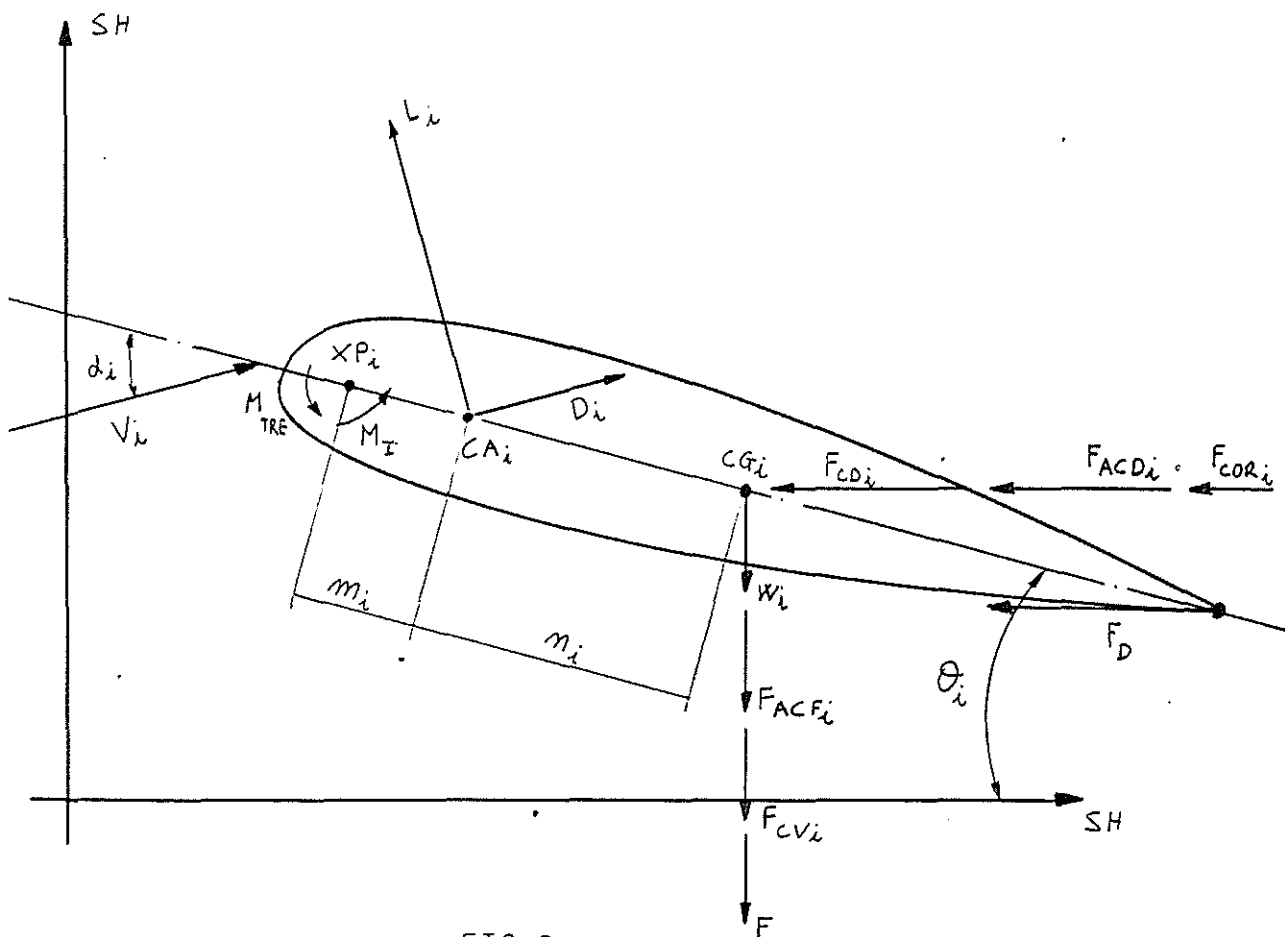


FIG. 3

For example:

$$1) \quad \vec{V}_{NF} = [A] * \vec{V}_{SH}$$

V_{SH} is the vector of the three components of flight speed referred to "SHAFT AXIS" provided, as we have said, as INPUTS

Another very important frame system is the "BLADE" one; at this system are referred the aerodynamic forces created by the rotor.

If β_{NF} is the flapping angle in the "NO-FEATHER" system we can write, in the classical way:

$$2) \quad \beta_{NF} = a_{0NF} - a_{1NF} \cos \psi - b_{1NF} \sin \psi$$

where:

$$\psi = \omega t = \text{AZIMUTH angle}$$

now we are able to calculate the components of speed in the "BLADE" system (refer to FIG. 1).

$$3) \quad \left\{ \begin{array}{l} V_{XBL} = V_{XNF} \sin \psi - V_{YNF} \cos \psi + \omega r \\ V_{YBL} = (V_{YNF} \sin \psi + V_{XNF} \cos \psi) \cos \beta_{NF} + \\ \quad (V_{ZNF} - V_{iNF}) \sin \beta_{NF} \\ V_{ZBL} = -(V_{YNF} \sin \psi + V_{XNF} \cos \psi) \sin \beta_{NF} + \\ \quad (V_{ZNF} - V_{iNF}) \cos \beta_{NF} - V_f \end{array} \right.$$

where:

V_{XNF} ; V_{YNF} ; V_{ZNF} = components of speed in the NF system evaluated with 1)

r = local position along the blade

V_{iNF} = induced velocity

V_f = speed induced by flapping motion = $\dot{\beta} r$

Naturally in equations 3) β_{NF} , V_{iNF} and V_f are

unknown and we must calculate them iteratively because each of these parameters affects the others and the forces created by the rotor.

When the above variables are calculated it becomes possible to write the elementary contribution of each blade element to the three forces and to the flapping and lagging moments about flap and drag hinges.

Indicating with:

n_B = number of blades

$$V_{TBL} = \sqrt{V_{XBL}^2 + V_{YBL}^2 + V_{ZBL}^2}$$

$\alpha(r, \psi)_{BL} \approx \alpha(r, \psi)_{NF}$ = angle of attack

$\theta_{NF} = \theta_0$ = geometric pitch in the "NF" system
(collective pitch)

$\varphi(r, \psi)_{NF} = \alpha_{NF} - \theta_{NF}$ = local angle of inflow

$c(r)$ = local chord

$S(r)$ = local twist

we have, with a little approximation:

$$4) \quad \alpha(r, \psi)_{NF} = \theta_0 + \text{Atn}[V(r, \psi)_{ZBL} / V(r, \psi)_{XBL}] + \\ [S(r) - S(0.75R)]$$

where the control angles are referred to the blade station placed at the 75% of the radius.

Calculated $\alpha(r, \psi)_{BL}$, and known in tabular form the aerodynamic characteristics of the airfoils distributed along the blade: $C_L(r, \psi, mach)$, $C_D(r, \psi, mach)$, $C_M(r, \psi, mach)$ it can be evaluated:

$$5) \quad dT_{NF} = \\ = 0.5n_B \rho v^2(r, \psi)_{TBL} c(r) [C_L \cos \varphi_{NF} + C_D \sin \varphi_{NF}] \\ \cos \beta_{NF} dr$$

$$6) \quad dH_{NF} = \\ = 0.5n_B \rho v^2(r, \psi)_{TBL} c(r) [(C_D \cos \varphi_{NF} - C_L \sin \varphi_{NF}) \\ \sin \psi - (C_L \cos \varphi_{NF} + C_D \sin \varphi_{NF}) \sin \beta_{NF} \cos \psi] dr$$

$$7) \quad dY_{NF} = \\ = 0.5n_B \rho v^2(r, \psi)_{TBL} c(r) [(-C_L \cos \varphi_{NF} - C_D \sin \varphi_{NF}) \\ \sin \beta_{NF} \sin \psi - (C_D \cos \varphi_{NF} - C_L \sin \varphi_{NF}) \cos \psi] dr$$

$$8) \quad dQ_{NF} = 0.5n_B \rho v^2(r, \psi)_{TBL} c(r) r \\ [C_D \cos \beta_{NF} \cos \varphi_{NF} - C_L \cos \beta_{NF} \sin \varphi_{NF}] dr = \\ = dQ_P - dQ_I$$

$$9) \quad dM_{FL} = 0.5 \rho v^2(r, \psi)_{TBL} c(r) r \\ [C_L \cos \varphi_{NF} + C_D \sin \varphi_{NF}] dr$$

where:

T_{NF} = thrust in the NF system

H_{NF} = H-force (in the X direction of NF system)

Y_{NF} = Y-force (in the Y direction of NF system)

Q_I = induced torque

Q_P = profile torque

Q_{NF} = total torque in NF system

M_{FL} = moment about flapping hinge

A double integration in r and ψ (average process) permits the calculation of the total forces and torque in the NF system.

2.2 FLAPPING MOTION

The calculation of flapping motion use the classical linearized differential equation:

$$10) \quad \ddot{\beta}_{NF} + \omega^2(1 + \epsilon) \beta_{NF} = M_{FL} / J_{FL}$$

where:

$$\epsilon = M_{BL} e x_{CG} R^2 / J_{FL}$$

e = offset of flapping hinge in percent of R

x_{CG} = blade center of gravity offset in percent of R

J_{FL} = flapping moment of inertia

M_{BL} = blade mass

β_{NF} = flapping angle in NF system

This equation can be resolved imposing that eq. 2) is a solution of eq. 10) in twenty different azimuthal locations. At these azimuthal locations it can be evaluated M_{FL} (eq.9) by simple integration in r.

The solution of a system of twenty equations in three unknown (a_{0NF} , a_{1NF} , b_{1NF}) allows the estimation of the three flapping coefficients.

The found flapping coefficients can be written in the "SHAFT" system by the simple and well known equations:

$$11) \quad \begin{cases} a_{0SH} = a_{0NF} \\ a_{1SH} = a_{1NF} + \theta_{90} \\ b_{1SH} = b_{1NF} - \theta_{00} \end{cases}$$

In writing these equations we have expressed the control pitch angle in the "SHAFT" system using the relation:

$$12) \quad \theta_{SH} = \theta_0 + \theta_{00} \cos \psi + \theta_{90} \sin \psi$$

2.3 LAGGING MOTION

As already seen for the flapping motion the lagging motion can be evaluated using the classical differential equation:

$$13) \quad \ddot{\eta} + (K / J_{DR}) \dot{\eta} + (\omega^2 \epsilon_{DR} + R_{DR} / J_{DR}) \eta = \\ = N_A / J_{DR} + 2 \beta \dot{\beta} \omega$$

with:

$$\epsilon_{DR} = M_{BL} e_{DR} x_{CG} R^2 / J_{DR}$$

e_{DR} = offset of lagging hinge in percent of R

J_{DR} = lagging moment of inertia

$$\eta = \text{lagging angle} = c_0 - c_1 \cos \psi - d_1 \sin \psi$$

K = damping characteristic of an eventual damper

R_{DR} = eventual stiffness of drag hinge

N_A = aerodynamic moment about drag hinge

$2 \beta \dot{\beta} \omega$ = dynamic coupling between **FLAPPING** and **LAGGING** motions due to the forces of **CORIOLIS**

In η calculation we have supposed that the intrinsic damping due to aerodynamic forces can be neglected and that the characteristic of the damper could be thought linear.

If:

$$14) N_A(\psi) = 0.5 \rho \int_{eR}^R (C_L \sin \varphi_{NF} - C_D \cos \varphi_{NF})^2 v_{TBL}^2(r, \psi) c(r) r dr$$

the eq. 13) can be resolved with the same procedure underlined for flapping motion.

3. THE INDUCED VELOCITY

For performances estimation we can leave out of account the induced velocity distribution on the rotor disk (**uniform down-wash**); the same thing cannot be done if we want to investigate about rotor dynamic or torsional loads at the blade root.

The PGM **NFCILL** was endowed with **MANGLER** and **SQUIRE** inflow model that, after accurate analysis, seems to be the most useful presently available.

MANGLER and **SQUIRE** inflow ditribution is a very complex function of azimuth angle and local radial position r ; it depends, moreover, on the disk angle of attack.

4. CALCULATION OF THE TORSIONAL MOMENTS AT THE BLADE ROOT

According to the methodology above described at each blade element are applied all the loads that give contribution to the moments around the blade pitch axes.

These loads, integrated along the radius, give, for a fixed blade azimuth angle, the total value of the torsional moment at the blade root.

4.1 IDENTIFICATION OF THE APPLIED LOADS

The loads on each blade element can be distinguished as follows:

- AERODYNAMIC LOADS
- INERTIAL LOADS
- LOADS DUE TO BLADE WEIGHT
- LOADS DUE TO THE LEAD-LAG DAMPER

Once determined, according to the method described in chapters 2 and 3, the blade motion and the local angle of attack, it is possible to evaluate the aerodynamic and inertial loads. The loads due to the weight are determined by the mass distribution along the blade span.

The calculations do not need, now, an iterative process and so are performed in the "SHAFT REFERENCE SYSTEM".

The reference point for the blade element moments (>0 nose up) is the local pitch axis position (XP_i in Fig.3).

4.2 AERODYNAMIC LOADS

Referring to Fig. 3 it will be:

$$15) \quad M_{Li} = - \int v_i^2 c_i c_{Li} \Delta r_i \cos \alpha_i m_i / 2$$

$$16) \quad M_{Di} = - \int v_i^2 c_i c_{Di} \Delta r_i \sin \alpha_i m_i / 2$$

$$17) \quad M_{Ai} = \int v_i^2 c_i^2 c_{Mi} \Delta r_i / 2$$

where:

$$\alpha(r, \psi) = \text{local angle of attack}$$

The aerodynamic forces are applied to the local aerodynamic center of the section (CA_i in Fig.3).

4.3 LOADS DUE TO THE WEIGHT

Referring again to Fig. 3 it will be:

$$18) \quad M_{Wi} = \int_i \Delta r_i g (m_i + n_i) \cos \theta_i$$

where:

θ_i = local blade pitch (including twist contribution)

g = acceleration of gravity

\int_i = mass for unit of length of the i_{th} blade element

4.4 INERTIAL LOADS

The following moments (acting on each blade element) due to the blade motions have been considered:

- MOMENT due to the blade pitch change: M_I
- MOMENT due to the blade flapping acceleration: M_{ACFi}
- MOMENT due to the blade lagging acceleration: M_{ACDi}
- MOMENT given by the coupling between flapping angle and centrifugal force: M_{CFi}
- MOMENT given by the coupling between lead-lag angle and centrifugal force: M_{CDi}
- MOMENT due to **TENNIS RACKET EFFECT**: M_{TREi}
- MOMENT due to the Coriolis forces : M_{CORi}

All the forces giving the moments above mentioned are applied to the centre of gravity of each blade element (CG_i in Fig.3).

4.4.1 MOMENT DUE TO THE CYCLIC BLADE PITCH CHANGE

If:

$$\theta_i(\psi) = \theta_0 + \theta_{00} \cos \psi + \theta_{90} \sin \psi + (S_i - S_{75})$$

will be:

$$19) \quad M_I(\psi) = - I_P \ddot{\theta}(\psi)$$

where:

I_P = pitch moment of inertia of the blade

$M_I(\psi)$ does not depend on the position along the span and will be evaluated only as a function of the blade azimuth.

4.4.2 MOMENT DUE TO THE BLADE FLAPPING ACCELERATION

Is:

$$20) \quad M_{ACFi}(\psi) = \ddot{\beta} r_i (m_i + n_i) \cos \theta_i \delta_i \Delta r_i$$

4.4.3 MOMENT DUE TO THE BLADE LAGGING ACCELERATION

Is:

$$21) \quad M_{ACDi}(\psi) = - \ddot{\eta} r_i (m_i + n_i) \sin \theta_i \delta_i \Delta r_i$$

4.4.4 MOMENT GIVEN BY THE COUPLING BETWEEN FLAPPING ANGLE AND CENTRIFUGAL FORCE

Fig. 4 shows the origin of this coupling:

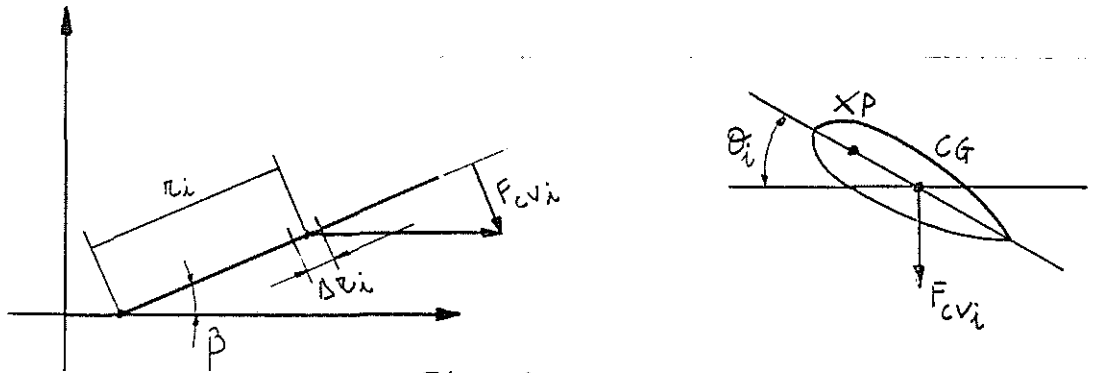


Fig. 4

$$22) F_{CVi}(\psi) = \sum_i \Delta r_i \omega^2 (e + r_i \cos \beta) \sin \beta$$

$$23) M_{CFi}(\psi) = F_{CVi} (m_i + n_i) \cos \theta_i$$

4.4.5 MOMENT GIVEN BY THE COUPLING BETWEEN LAGGING ANGLE AND CENTRIFUGAL FORCE

Fig. 5 shows the origin of this coupling:

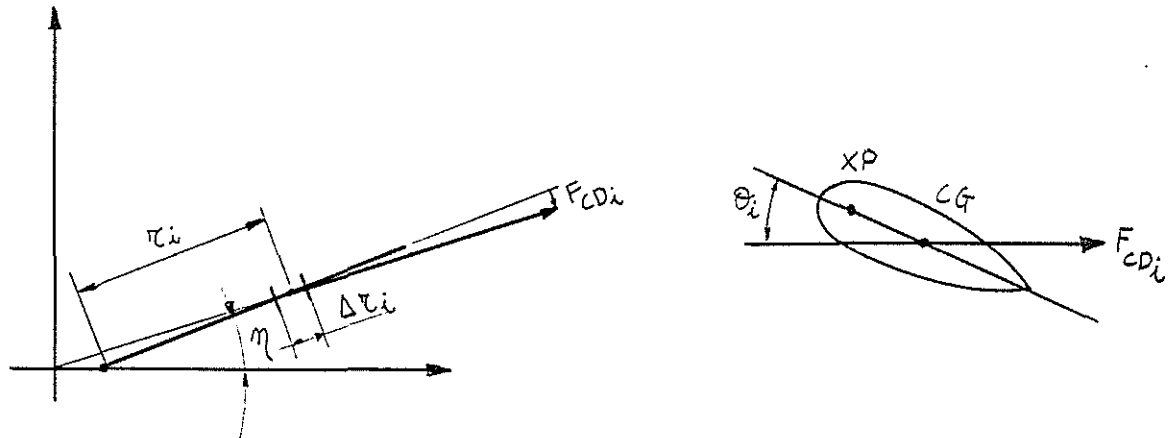


Fig. 5

$$24) F_{CDi}(\psi) = \sum_i \Delta r_i \omega^2 r_i \sin \eta$$

$$25) M_{CDi}(\psi) = - F_{CDi} (m_i + n_i) \sin \theta_i$$

4.4.6 TENNIS RACKET EFFECT

The tennis racket effect has been evaluated in a simple way under the hypothesis that the chord distribution of each blade element mass can be represented by two masses placed at fixed distance from the centre of gravity.

The modelling used to calculate the T.R.E. is shown in Fig. 6.

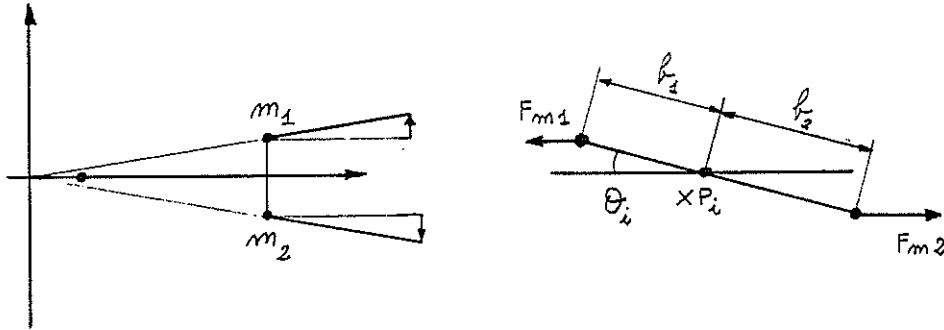


Fig. 6

$$26) M_{TREi}(\psi) = - (F_{m1i}b_1 + F_{m2i}b_2)\sin \theta_i$$

4.4.7 MOMENT DUE TO THE CORIOLIS FORCE

This effect is due to the coupling arising from flapping velocity and rotor angular speed (fig. 7):

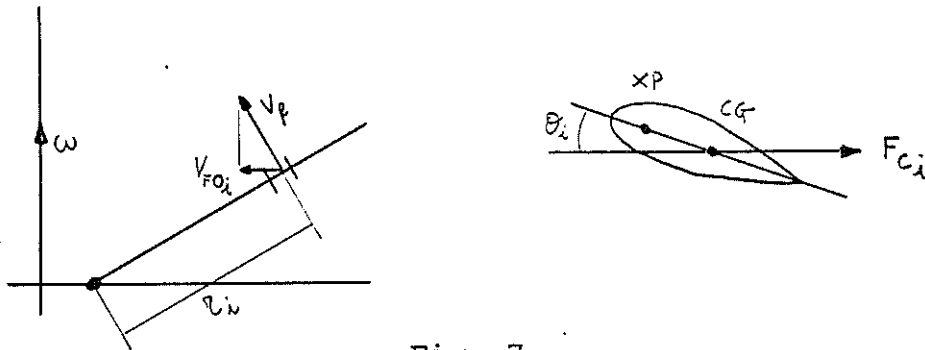


Fig. 7

$$27) v_{FOi} = \dot{\beta} r_i \sin \beta_i$$

$$28) a_{COR} = 2\omega \wedge v_{FOi} = 2\omega v_{FOi}$$

$$29) M_{CORi}(\psi) = -2\delta_i \Delta r_i \omega v_{FOi} (m_i + n_i) \sin \theta_i$$

5. LOADS DUE TO THE LEAD-LAG DAMPER

Starting from the damper geometry and its blade attachment points and having determined the lead-lag motion, it is possible to evaluate the loads at the blade root (Fig. 8)

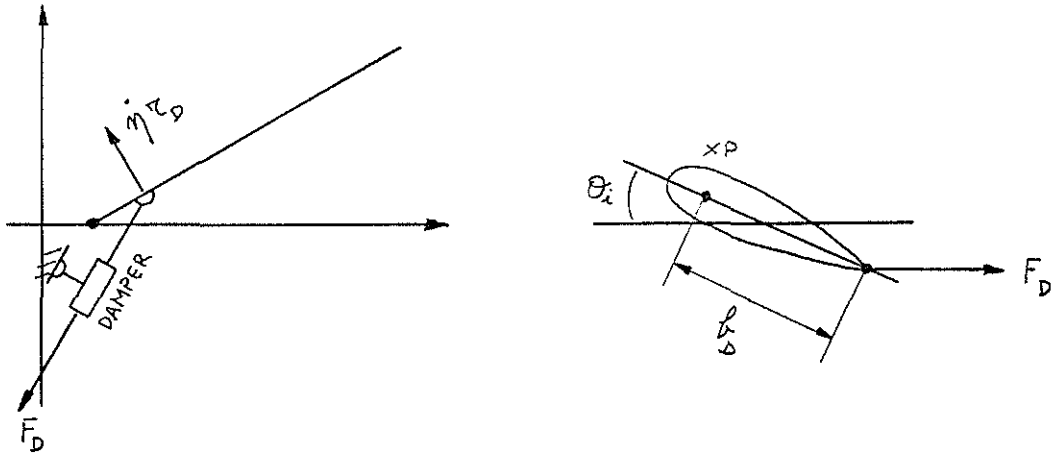


Fig. 8

$$30) \quad M_D(\psi) = -F_D b_D \sin \theta_i$$

This formulation is approximate, but from a practical point of view, its accuracy has been demonstrated to be acceptable.

6. UNSTEADY AERODYNAMIC

Due to the pitching and heaving of the blade sections, the calculation of the aerodynamic characteristics must take into account the unsteady effects.

For the present calculation is particularly significant the evaluation of the effect of unsteady aerodynamics on the pitching moment coefficient of airfoils.

In the code **NFCTLL** has been developed a routine for the calculation of the unsteady aerodynamic coefficients based on **ERICSSON** theory (see Ref. 1).

7. COMPARISON WITH EXPERIMENTAL DATA

The above described method has been tested comparing its results with the available flight test data of A129 and EH-101.

The code has been, also, compared with the results of more sophisticated methods using the working example rotor ORMISTON.

The analysis is performed under the following assumptions:

- Induced velocity distribution according to Mangler and Squire theory.
- Unsteady aerodynamics

The comparison with the A129 flight tests data is shown in Fig. 9-10-11 and refers to speeds of 0-60-130 Kts.

The comparison concerning the EH-101 data is summarized in Fig. 12-13-14-15-16-17 and the corresponding speeds are 100-110-120-130-140-150 Kts.

The comparisons are developed in a qualitative way and the results are expressed in percentage of the maximum peak value measured in flight at the given condition.

In Fig. from 18 to 24 is shown the comparison with the ORMISTON rotor.

7.1 A129

In hover the steady value shows a good correlation, the wave form is very different from the measured one. This is due to the fact that the code NFCTLL does not take into account the blade vortex interactions and the interferences between main rotor - tail rotor and main rotor - fuselage; anyway the results are in good accordance with the measured values.

At 60 Kts the program overestimates the compression peak; the tension peak is, on the contrary, well estimated.

The wave form shows a good correlation and the overestimation of the negative peak is considered acceptable.

At 130 Kts the negative peak is slightly underestimated, while, the positive one is well predicted; the wave form appears rather good.

7.2 EH-101

The blade of EH-101 is not a conventional blade because of its planform and airfoils distribution. The comparison between calculations and flight test data appears, for this reason, very important.

It has to be underlined that the measured data could be affected by some problems due to the youth of the helicopter.

At 100 kts NFCTLL code well estimates the compression load but it underestimates the measured tension load.

At 110 Kts remains the underestimation of the tension load and it has to be noticed the lack of the little compression load present in the experimental data.

At 120 Kts the comparison between measured and calculated data appears quite good.

At 130-140-150 Kts NFCTLL program does not find the compression loads present in the flight test data, the tension loads appear, on the contrary, always estimated with good approximation.

On the whole the results have to be considered satisfactory.

7.3 ORMISTON ROTOR

In Fig. from 18 to 24 is shown that the NFCTLL evaluation of thrust, torque, flapping and control angles is in accordance with the results of the others codes used for the comparison.

The oscillatory torsional loads at the blade root, estimated with the methodology above described, are in agreement with the results of others more complex and sophisticated computer programs.

8. CONCLUSIONS

The methodology here proposed, based on simplified approach, gives good results and allows to evaluate the pitch link loads with acceptable accuracy.

For this reason it is very useful during the preliminary design phase where can be appreciated its characteristics of:

- low execution time (\sim 30 sec CPU time on a IBM 3083 computer)
- reduced input data
- cost effectiveness of the code used for parametric studies

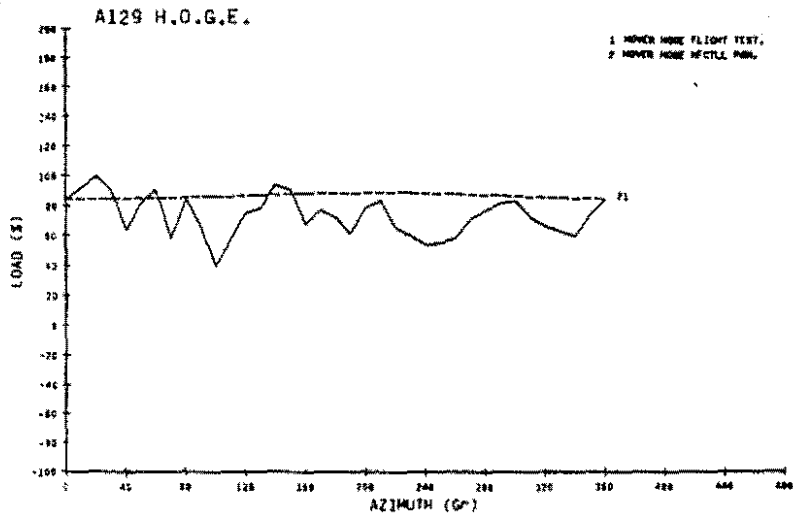


FIG. 9

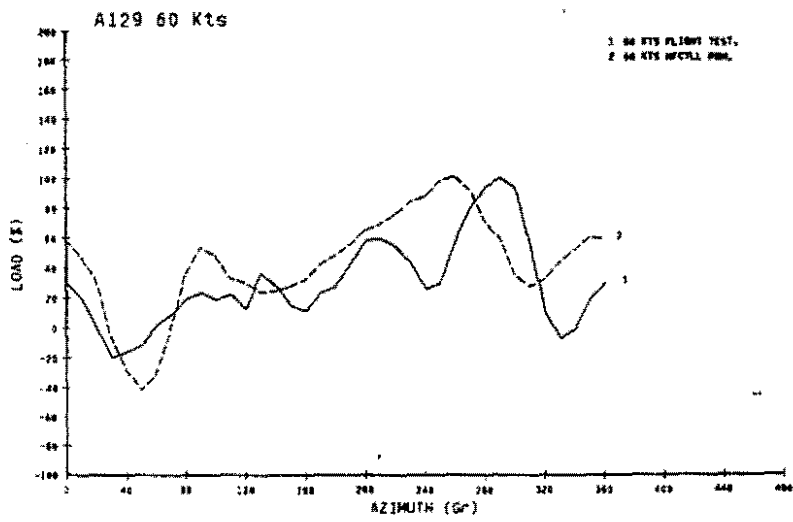


FIG. 10

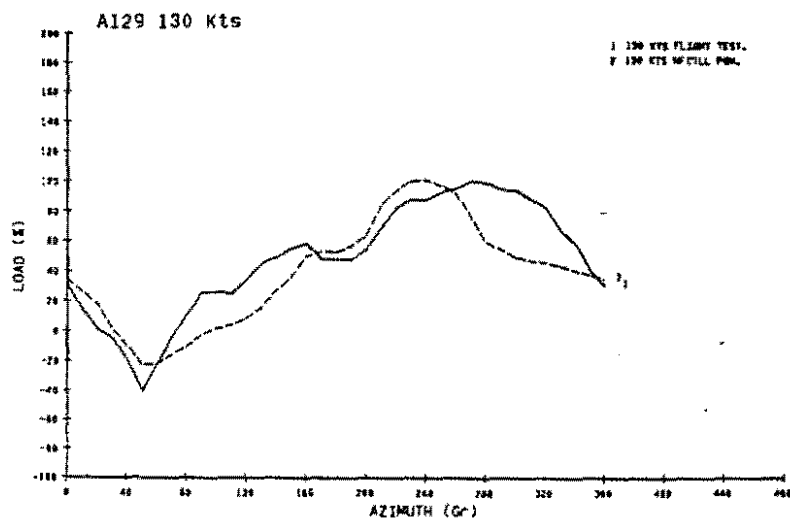


FIG. 11

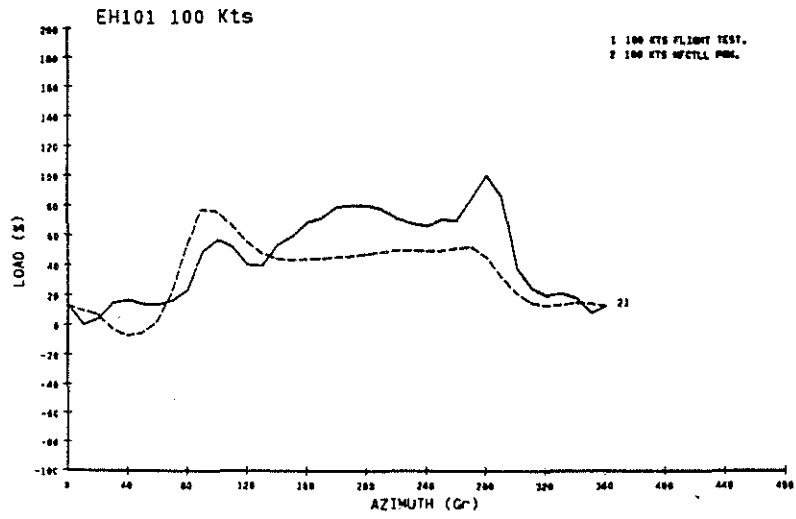


FIG. 12

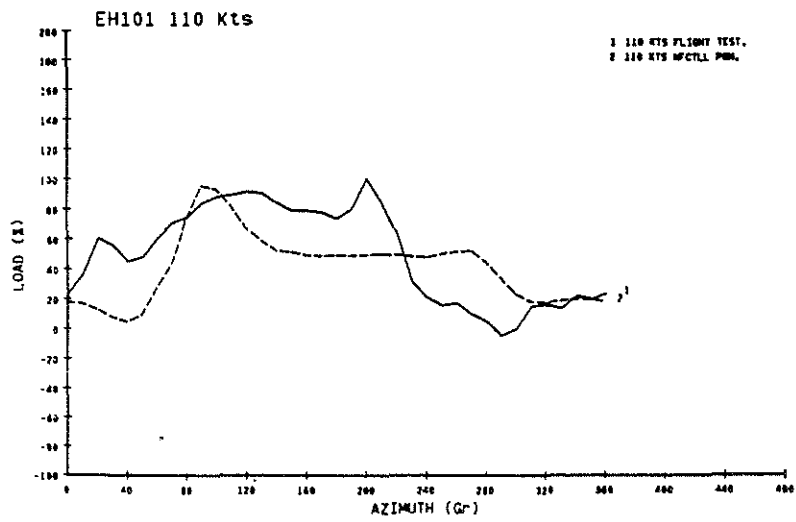


FIG. 13

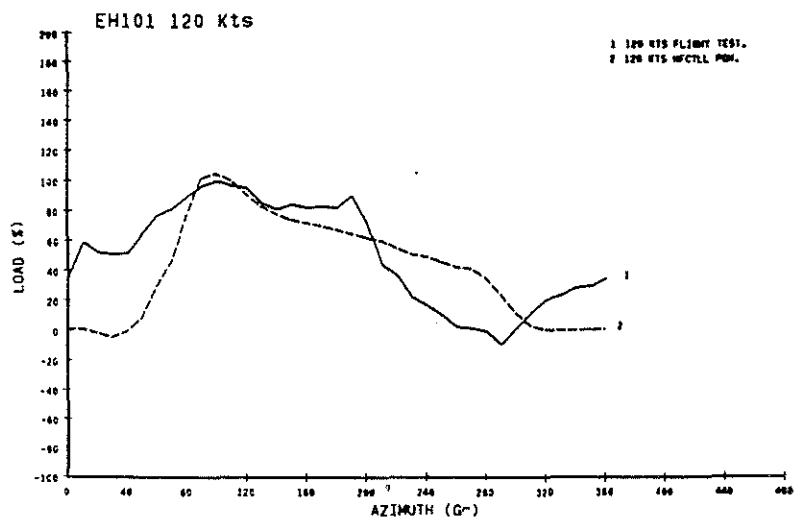


FIG. 14

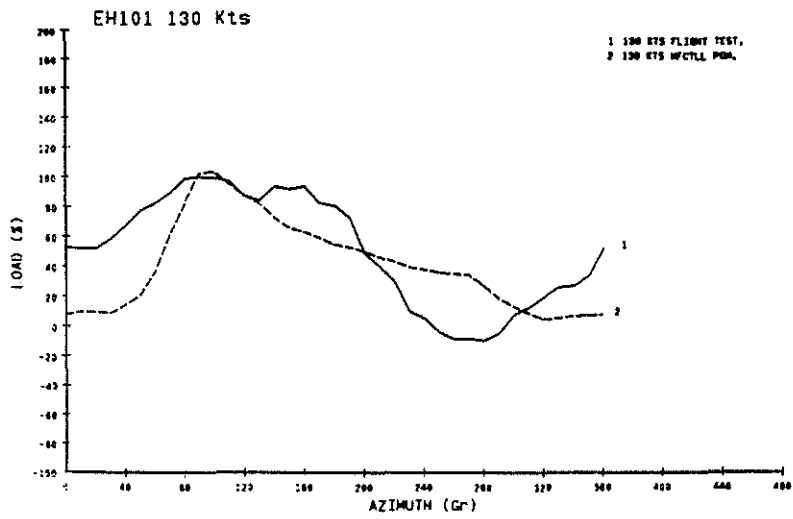


FIG. 15

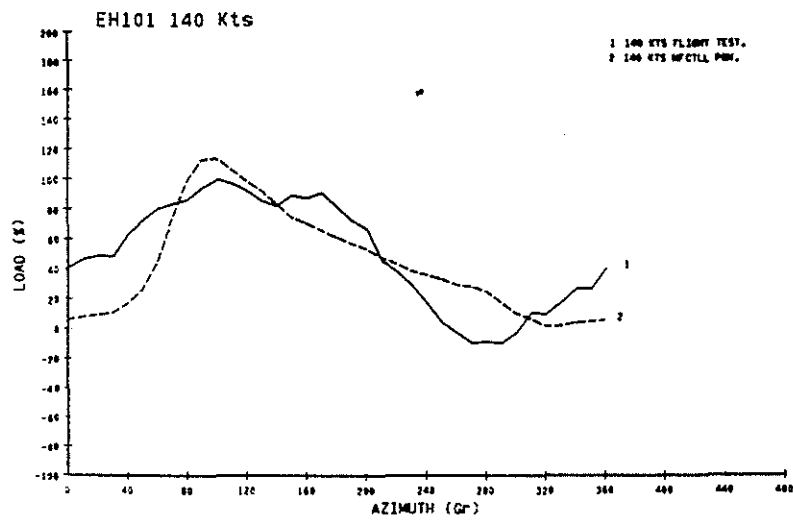


FIG. 16

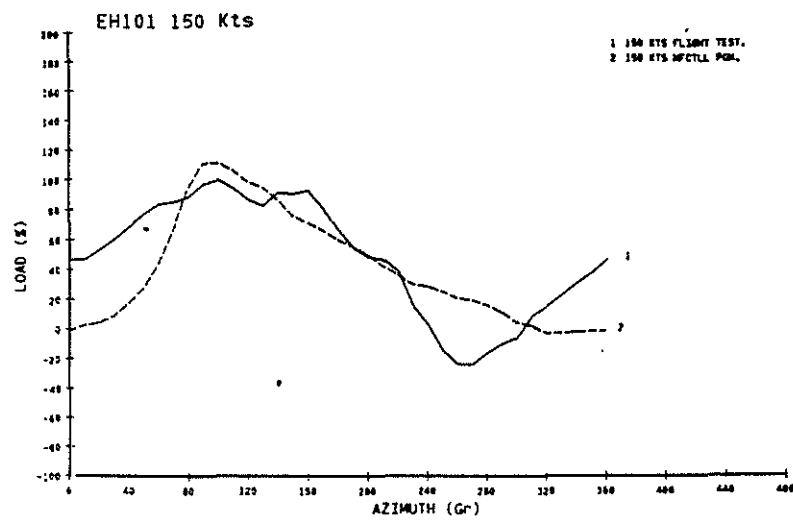


FIG. 17

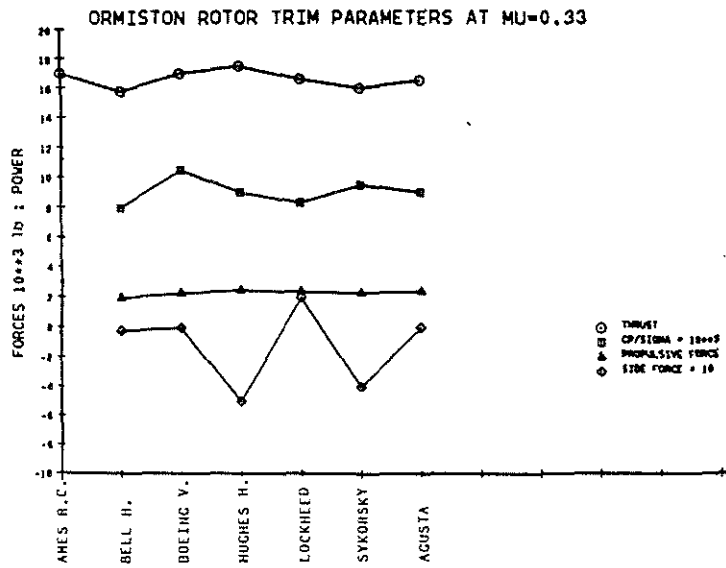


FIG. 18

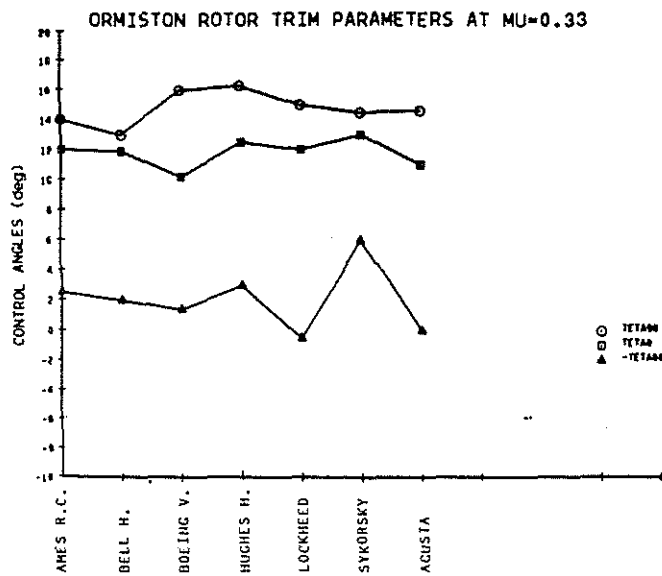


FIG. 19

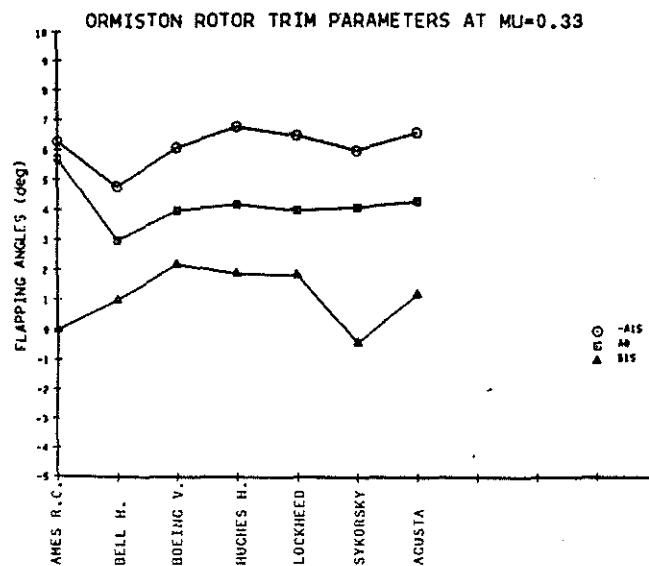


FIG. 20

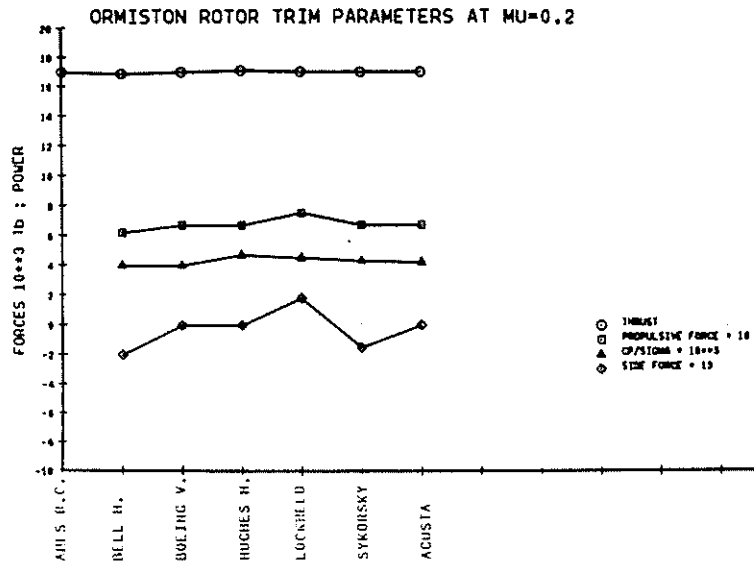


FIG. 21

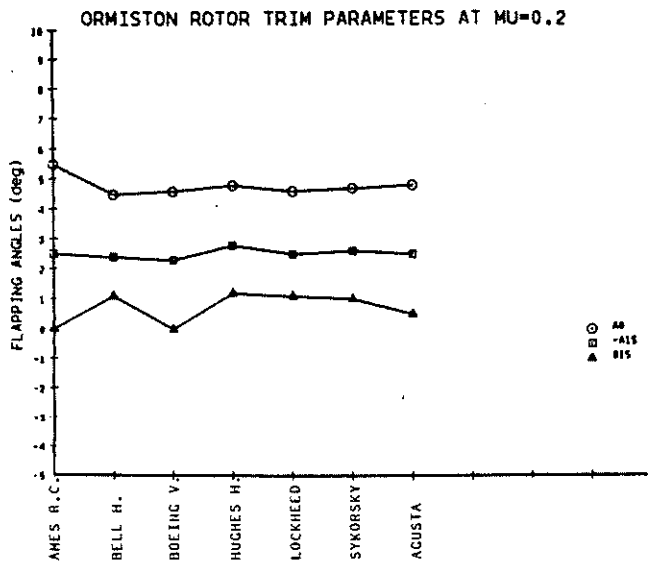


FIG. 22

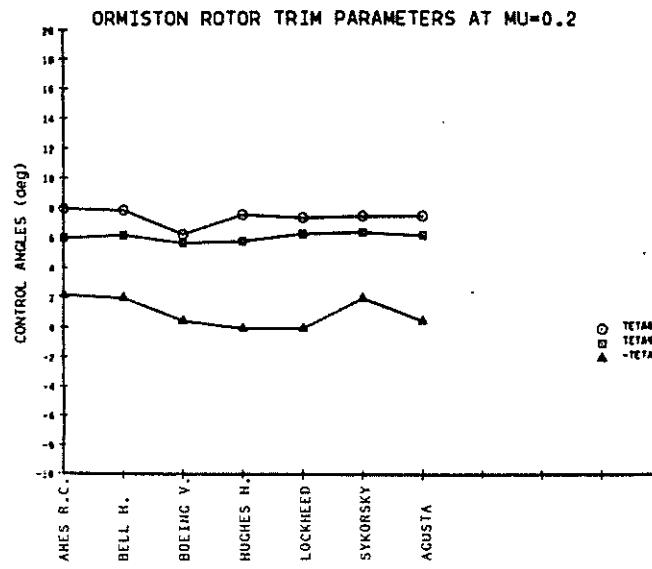


FIG. 23

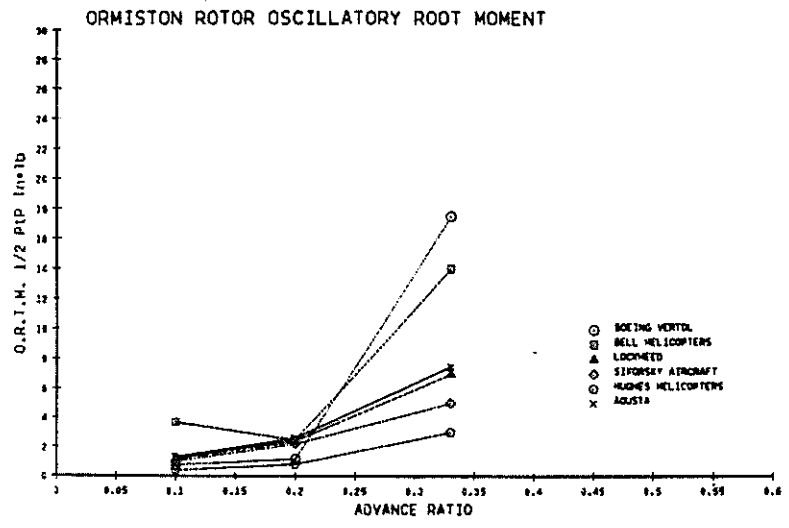


FIG. 24

REFERENCES

1. L. E. Ericsson and J. P. Reding "Unsteady airfoil stall, review and extension" presented at the AIAA VIII Aerospace Sciences Meeting, January 1970.
2. R. A. Ormiston "Comparison of several methods for predicting loads on a hypothetical helicopter rotor" presented at the AHS/NASA-Ames Specialist's Meeting on Rotorcraft Dynamics, February 1974.
3. A. R. S. Bramwell "Helicopter Dynamics" - Edward Arnold Publishers Ltd 25 Hill St, London W1X 8LL
4. R. W. Prouty "Helicopter Performances, Stability, and Control" - PWS Engineering Boston.
5. F. Nannoni "Guida Utente al Programma NFCTLL" - Agusta internal report, January 1988.